Dynamical mass generation in QED₃ beyond the instantaneous approximation[*]

Hai-Xiao Xiao(肖海校)[1]   Jian-Feng Li(李剑锋)[1,2]   Wei Wei(魏巍)[1]

Pei-Lin Yin(尹佩林)[3]   Hong-Shi Zong(宗红石)[1,4,5;1]

[1] Department of Physics, Nanjing University, Nanjing 210093, China
[2] College of Mathematics and Physics, Nantong University, Nantong 226019, China
[3] Department of Physics, Southeast University, Nanjing 211189, China
[4] Joint Center for Particle, Nuclear Physics and Cosmology, Nanjing 210093, China
[5] State Key Laboratory of Theoretical Physics, Institute of Theoretical Physics, Chinese Academy of Sciences, Beijing 100190, China

Abstract: In this paper, we investigate dynamical mass generation in (2+1)-dimensional quantum electrodynamics at finite temperature. Many studies are carried out within the instantaneous-exchange approximation, which ignores all but the zero-frequency component of the boson propagator and fermion self-energy function. We extend these studies by taking the retardation effects into consideration. In this paper, we get the explicit frequency n and momentum p dependence of the fermion self-energy function and identify the critical temperature for different fermion flavors in the chiral limit. Also, the phase diagram for spontaneous symmetry breaking in the theory is presented in T_c-N_f space. The results show that the chiral condensate is just one-tenth of the scale of previous results, and the chiral symmetry is restored at a smaller critical temperature.

1   Introduction

(2+1)-dimensional quantum electrodynamics (QED₃) has been long investigated for its many interesting characteristics, like confinement and dynamical chiral symmetry breaking (DCSB). Confinement and DCSB are believed to be crucial in understanding Quantum Chromodynamics (QCD). As a non-Abelian gauge theory with asymptotic character, however, it is hard to gain much insight into these features by conventional methods, like perturbative methods. As a result, QED₃ can be a good alternative to investigate these interesting characteristics to help us understand QCD. Among these studies, the Dyson-Schwinger equations (DSEs) are one of the most widely used tools [1–4].

QED₃ has also been studied for possible applications in condensed matter systems, like high-T_c cuprate superconductors [5–16] and graphene [17–22]. High-T_c cuprate superconductors have an unconventional d-wave symmetry of the pairing condensate. There are nodes on the pairing gap at the Fermi surface, and its low-energy dispersion becomes linear and thus can be described as massless fermions. The motion of the modes is mainly confined within the two-dimensional copper-oxygen planes, so it suggests the low-energy behavior of these systems can be described in terms of a quantum electrodynamics in two spatial dimensions with two massless fermion flavors [11, 12, 14, 23, 24]. In this picture the antiferromagnetically ordered insulating state of the cuprates would correspond to a state of broken chiral symmetry. For this reason, it is also meaningful to study DCSB in (2+1)-dimensional quantum electrodynamics.

In the past few decades, the chiral phase transition in QED₃ at zero temperature has aroused great interest and been investigated intensively. T.W. Appelquist et al. [25] first solved the DSE for the fermion self-energy function, within the approximation that keeps only the leading-order contribution in $1/N_f$ expansion, and found that the chiral phase transition takes place only when the number of fermion flavors is smaller than a critical $N_f^c = 32/\pi^2$. D. Nash [26] gave a critical number of fermion flavors $N_f^c = 128/3\pi^2$ by further taking into account the next-to-leading-order corrections to fermion wave-function renormalization function. These results have been questioned in Refs. [27, 28], where they argued that the $1/N_f$ expansion is not an appropriate tool to ad-

dress these nonpeturbative phenomena. Using a slightly different truncation of the fermion DSE, they found that chiral symmetry is broken for all values of N_{f}, although the generated mass scale exponentially decreases for increasing N_{f}. Later, P. Maris [29] investigated this problem in a different way by solving a set of coupled integral equations for the fermion wave-function renormalization function, the fermion self-energy function, and the boson vacuum polarization within a range of simplified fermion-boson vertexes, and arrived at a critical number of fermion flavors $N_{\mathrm{f}}^c = 3.3$. This result puts an end to the argument of the existence of a critical number of fermion flavors. Subsequently, C.S. Fischer et al. [30] employed an ansatz satisfying the Ward-Takahashi identity for the fermion-boson vertex to get a more accurate numerical value of N_{f}^c and found a critical number of fermion flavors $N_{\mathrm{f}}^c \approx 4$.

Since many physical systems have interesting phenomena and physical properties at finite temperature, it is interesting to investigate DCSB in QED$_3$ at finite temperature. Due to the Coleman-Mermin-Wagner theorem [31, 32], continuous symmetries cannot be spontaneously broken at finite temperature in systems with sufficiently short-range interactions in dimensions $D \leqslant 2$. Furthermore, as mentioned above, many experimental results show that high-T_{c} cuprate superconductors have plane conducting characteristics, which means the motion of the carriers is mainly in the CuO_2 plane. More accurate experiments show that the critical temperatures for high-T_{c} cuprate superconductors with different numbers of layers are different. With the number of layers increasing from one to a certain number, the critical temperature increases. When the number of layers reaches a certain value, the critical temperature shows a tendency to decrease as the number of layers increases [33, 34]. This shows that in reality the inter-layer coupling has a practical effect on the in-plane physical systems. As a matter of fact, the inter-layer coupling can easily drive the system into a true ordered state once the in-plane correlations are already strong, e.g., below the mean field transition temperature. Usually, the DCSB in QED$_3$ at finite temperature is studied by a self-consistent calculation of DSE in the rainbow approximation in QED$_3$, which is like the mean field theory in condensed matter physics. In such a theory, the correlation between fluctuations of the order parameter is ignored. Nevertheless, the mean field transition temperature provides a correct energy scale below which the amplitude of the order parameter becomes finite and its spatial correlation becomes strong and rather long-ranged. In this sense, the mean field transition marks a crossover in the thermodynamic properties. In particular, for a $U(1)$ or $O(2)$ symmetry to be broken, there is in fact an algebraic order below the so-called Kosterlitz-Thouless (KT) transi-

tion temperature (the transition can be found in several 2-D systems in condensed matter physics that are approximated by the XY model, including Josephson junction arrays and thin disordered superconducting granular films; more recently, the term has been applied by the 2-D superconductors insulator transition community to the pinning of Cooper pairs in the insulating regime, due to similarities with the original vortex KT transition), a temperature not far from the mean field one.

In this paper, we mainly concentrate on dynamical gap generation in QED$_3$ at finite temperature. Many studies have been done in related areas. In 1987, Kocic first found that there is a critical temperature T_{c} above which chiral symmetry is restored, using a very simple approximation solving the finite temperature Dyson-Schwinger equations (DSEs) [35]. Later, N. Dorey et al. had made some improvements on investigating DCSB in QED$_3$ at finite temperature and discussed the relevance to high-T_{c} superconductors [36, 37]. This problem was carried out by solving the DSEs of fermions within the formalism of the imaginary time Matsubara Green's function. For simplicity, their work was carried out with a few approximations to get a qualitative result. These included replacing the full fermion-boson vertex Γ_ν by the bare fermion-boson vertex and neglecting the fermion wave-function renormalization effect, and the photon polarization function was calculated considering only the one-loop contribution. Since this truncation scheme helps to keep the gauge-invariance of the DSEs, it is widely used in investigating DCSB at zero temperature [25–30]. In order to avoid the computation complexity, the fermion self-mass Σ was taken to depend on temperature only, not on momentum and energy explicitly. They got the temperature dependence of the dynamically generated mass gap, and found that dynamical mass gap generation is suppressed at finite temperature and the dynamically generated mass gap vanishes above a certain critical temperature T_{c} ($T_{\mathrm{c}} = 4.9 \times 10^{-2}\alpha$ for $N_{\mathrm{f}} = 1$). The fermion self-mass varies as the momentum and energy change, so it is hard to know to what extent the result is reliable.

Subsequently, many studies have made an effort to improve the correctness of this calculation. In Ref. [38], I.J. Aitchison et al. further take the momentum dependence of the fermion self-energy and wave-function renormalization function into consideration. They got a non-physical result of $Z > 1$, even when the temperature approaches zero. They then proposed a modified equation and got a similar N_{f}-T phase diagram as in Ref. [37]. Later, they took the retardation effects and other parts of the photon propagator $\Delta_{\mu\nu}$ into consideration, but ignored the momentum dependence of fermion self-energy. They got numerical results for the temperature dependence of the dynamically generated mass [39]. Within

the instantaneous approximation and adopting a similar truncation scheme as in Ref. [37], one thorough study was done by Aitchison et al.. They extended the analysis of Ref. [36] by further considering the momentum dependence of the fermion self-energy function, and gave the temperature dependence of the fermion self-energy function and the chiral phase diagram at $N_{\rm f}$-T space [40]. Later, Feng et al. [41–43] investigated various properties of QED$_3$ at finite temperature and/or finite density, and made a thorough investigation of the phase structure of finite temperature QED$_3$.

Most recently, Yin et al. [44] extended this investigation and further considered the impurity potential effect on the chiral phase transition in thermal QED$_3$. They got a critical temperature $T_{\rm c}$=2.47×10^{-2}, at $N_{\rm f}$=2. Some other works concerning the temperature dependence of fermion self-mass have also been carried out in QED$_3$-like systems [45, 46]. Ref. [45] worked in the real-time formalism of finite field theory, and got a critical $T_{\rm c}$=5.4×10^{-4}, at $N_{\rm f}=2$. However, the results varied with the lattice size and cut-off change.

Some other studies concerning the temperature dependence of fermion self-mass has also been carried out in QED$_3$ like systems [45, 46]. Ref. [45] worked in the real-time formalism of finite field theory, and had given a critical $T_{\rm c}$=5.4×10^{-4}, at $N_{\rm f}$=2, but the results varied as the lattice size and cut-off change.

It is widely believed that the instantaneous approximation is valid at high temperature. But, as we know, dynamical gap generation is a low-energy phenomenon, so whether this approximation can give a reliable result in investigating dynamical gap generation in QED$_3$ remains unknown. Including the retardation effect will weaken the suppression effect of temperature or will further suppress the gap generation at finite temperature.

The paper is organized as follows. In Section 2, we discuss the DSE for the fermion self-energy function at finite temperature and then give the criteria for the chiral phase transition. In Section 3, we briefly present some critical details of the calculation and explore the finite temperature behavior of the vacuum polarization function, fermion self-energy function. Then, we give the $N_{\rm f}$ and T dependence of chiral condensate and chiral susceptibility and the phase diagram for spontaneous chiral phase transitions at $N_{\rm f}$-T. A brief summary and discussion are given in Section 4.

2   Dyson-Schwinger equations at finite temperature

2.1   Dyson-Schwinger equations in QED₃

In Euclidean space, the Lagrangian density of QED$_3$

with $N_{\rm f}$ flavors of massless fermions is given by

$$\mathfrak{L}=\sum_{f=1}^{N_{\rm f}}\bar{\psi}_{\rm f}(\slashed{\partial}+{\rm i}e\slashed{A})\psi_{\rm f}+\frac{1}{4}F_{\mu\nu}^2+\frac{1}{2\xi}(\partial_\mu A_\mu)^2. \quad (1)$$

The lowest rank irreducible representation of the Lorentz group is of two dimensions in (2+1)-dimensional space-time. In this representation, Dirac fermions are described by two-component spinors and the γ-matrices can be chosen as the usual Pauli matrices. However, as the three Pauli matrices are a complete set of mutually anticommuting 2×2 matrices, it is impossible to define an extra 2×2 matrix that anticommutes with all three γ-matrices. Consequently there is no extra matrix to generate a chiral symmetry that would be broken by a mass term $m\bar{\psi}\psi$, whether explicit or dynamically generated. In this paper, we employ the four-component spinors and 4×4 matrix representation of the Lorentz group. For the fermion propagator, the finite temperature version of DSE is given by

$$S^{-1}(p) = S_0^{-1}(p)-\frac{\alpha}{N_{\rm f}}\sum\!\!\!\!\!\!\int\gamma^\mu\times S(k)\Delta_{\mu\nu}(q)\Gamma_\nu(p,k), (2)$$

$$S_0^{-1}(p) = {\rm i}\vec{\gamma}\cdot\vec{p}+{\rm i}\gamma_3 p_3, \quad (3)$$

where $p = (p_3,\vec{p})$ with $p_3 = (2m+1)\pi T$ and $|\vec{p}| = P$, $k = (k_3,\vec{k})$ with $k_3 = (2n+1)\pi T$ and $|\vec{k}| = K$, and $q=(q_3,\vec{q})=p-k$ with $q_3=2(m-n)\pi T$ and $|\vec{q}|=Q=|\vec{p}-\vec{k}|$.

The notation $\sum\!\!\!\!\!\!\int$ denotes $\sum_{n=-\infty}^{+\infty}\int\frac{{\rm d}^2\vec{k}}{(2\pi)^2}$. $S^{-1}(p)$ and $S_0^{-1}(p)$ are the inverse of full and free fermion propagators at finite temperature; $\Gamma_\nu(p,k)$ is the full fermion-boson vertex; $\Delta_{\mu\nu}(q)$ is the full boson propagator at finite temperature. The coupling constant $\alpha = N_{\rm f}e^2$ has dimension one, thus providing us with a mass scale. In this paper the momentum, temperature and fermion self-energy are all measured in unit of e^2, namely, we choose natural units in which $e^2=1$.

Equation (3) forms an infinite hierarchy of integral equations for the Green's functions of the theory and some approximations are required for numerical calculation .

As stated in the introduction, we take the rainbow approximation, in which Γ^ν is replaced by its bare value $e\gamma^\nu$, work in the Landau gauge, and assume that the wave function renormalization is neglected. As a result, we can have $S^{-1}(p)=\slashed{p}+B(p)$, where $B(P,\beta)$ stands for the fermion self-energy function. The trace of Eq. (3) then yields a closed integral equation for $B(p)$:

$$B(p)=\frac{\alpha}{4N_{\rm f}}\int\frac{{\rm d}^3k}{(2\pi)^3}\times\frac{B(k)}{k^2+B^2(k)}{\rm Tr}[\gamma^\mu\Delta_{\mu\nu}(q)\gamma^\nu], \quad (4)$$

Subsequently, we can get the DSE for the fermion self-

energy function at finite temperature:

$$B_m(p,\beta)=\frac{\alpha}{N_f\beta}\sum\!\!\!\!\!\!\int\Delta(q,\beta)\times\frac{B_n(k,\beta)}{k^2+B_n^2(k,\beta)}, \quad (5)$$

with

$$\Delta(q,\beta)=\frac{1}{4}\mathrm{Tr}[\gamma^\mu\Delta_{\mu\nu}(q,\beta)\gamma^\nu]. \quad (6)$$

For the boson propagator, the finite temperature version of DSE is written as

$$\Delta_{\mu\nu}^{-1}(q) = \Delta_{\mu\nu}^{0,-1}(q)+\Pi_{\mu\nu}(q), \quad (7)$$

$$\Delta_{\mu\nu}^{0,-1}(q) = q^2(\delta_{\mu\nu}-q_\mu q_\nu/q^2), \quad (8)$$

$$\Pi_{\mu\nu}(q)=-N_f T \sum\!\!\!\!\!\int \mathrm{Tr}[\gamma_\mu S(k)\Gamma_\nu(p,k)S(p)], \quad (9)$$

where $\Delta_{\mu\nu}^{0,-1}(q)$ is the inverse of the free boson propagator and $\Pi_{\mu\nu}(q)$ is the vacuum polarization tensor.

As done in Ref. [37], we also decompose the vacuum polarization tensor in terms of two independent transverse tensors

$$\Pi_{\mu\nu}(q)=\Pi_A(q)A_{\mu\nu}+\Pi_B(q)B_{\mu\nu}, \quad (10)$$

where

$$A_{\mu\nu}=(\delta_{\mu 0}-\frac{q_\mu q_0}{q^2})\frac{q^2}{Q^2}(\delta_{\nu 0}-\frac{q_\nu q_0}{q^2}), \quad (11)$$

and

$$B_{\mu\nu}=\delta_{\mu i}(\delta_{ij}-\frac{q_i q_j}{Q^2})\delta_{j\nu}, \quad (12)$$

$A_{\mu\nu}$ and $B_{\mu\nu}$ are orthogonal and satisfy the following relationship

$$A_{\mu\nu}+B_{\mu\nu}=\delta_{\mu\nu}-\frac{q_\mu q_\nu}{q^2}. \quad (13)$$

The functions $\Pi_A(q)$ and $\Pi_B(q)$ are related to the temporal and spatial components of the vacuum polarization tensor $\Pi_{\mu\nu}(q)$ by the following expressions

$$\Pi_A=\frac{q^2}{Q^2}\Pi_{00}(q), \quad (14)$$

and

$$\Pi_B(q)=\Pi_{ii}(q)-\frac{q_0^2}{Q^2}\Pi_{00}(q). \quad (15)$$

Substituting Eqs. (8) and (10) into Eq. (7), we get an alternative expression for the full finite temperature boson propagator

$$\Delta_{\mu\nu}(q)=\frac{A_{\mu\nu}}{q^2+\Pi_A(q)}+\frac{B_{\mu\nu}}{q^2+\Pi_B(q)}. \quad (16)$$

Herein we follow Refs. [42–44] in retaining only the temporal component of the boson propagator, and then we get the approximate expression of the boson propagator:

$$\Delta_{\mu\nu}(q,\beta)=\frac{A_{\mu\nu}}{q^2+\Pi_A(q,\beta)}. \quad (17)$$

Substituting Eq. (17) into Eq. (6), we can get the iteration function for fermion self-energy function

$$B_m(p,\beta)=\frac{2\alpha}{N_f\beta}\sum\!\!\!\!\!\!\int\frac{B_n(p,\beta)}{k^2+B_n^2(p,\beta)}\frac{1}{q^2+\Pi_A(q,\beta)}, \quad (18)$$

To the leading-order contribution of $1/N_f$ expansion, the vacuum polarization function is given by

$$\Pi_{\mu\nu}(q)=-N_f T\sum\!\!\!\!\!\!\int\mathrm{Tr}[\gamma_\mu S_0(k)\Gamma_\nu(p,k)S_0(p)]. \quad (19)$$

Following the steps taken by Ref. [37], we can obtain the explicit expression for the vacuum polarization function at finite temperature:

$$\begin{aligned}\Pi_A(q,\beta) = &\frac{\alpha}{\pi\beta}\int_0^1 \mathrm{d}x\times\ln[4\cosh^2(\frac{1}{2}q\beta\sqrt{x(1-x)})\\&-4\sin^2(xm\pi)].\end{aligned} \quad (20)$$

2.2   Criteria for chiral phase transition

The chiral condensate is the vacuum expectation value of the scalar operator $\bar\psi\psi$. Its nonzero value indicates that chiral symmetry reflected on the Lagrangian level is spontaneously broken on the vacuum level and the chiral symmetry gets restored when the chiral condensate vanishes for the chiral limit. Due to this characteristic, chiral condensate is usually taken as the order parameter for the chiral phase transition.

The chiral condensate is commonly given by the first-order derivative of the generating functional with respect to the current mass of the fermion

$$\begin{aligned}\langle\bar\psi\psi\rangle(T) = &-\frac{\partial\ln Z}{\partial m}=-T\sum\!\!\!\!\!\!\int\mathrm{Tr}[S(p)]\\= &-4T\sum_{n=-\infty}^{\infty}\int\frac{\mathrm{d}^2 k}{(2\pi)^2}\frac{B_n(k,\beta)}{k^2+B_n^2(k,\beta)^2},\end{aligned} \quad (21)$$

where the notation Tr denotes trace operation over Dirac indices of the fermion propagator.

Susceptibility is defined as the first-order derivative of the order parameter. Usually the divergent or some other singular behaviors of the susceptibility are usually regarded as essential characteristics of phase transition [47–51].

Chiral susceptibility is defined as the first-order derivative of the chiral condensate with respect to the current mass of the fermion

$$\chi^c=-\frac{\partial\langle\bar\psi\psi\rangle(T)}{\partial m}=\frac{T}{V}\frac{\partial^2\ln Z}{\partial m^2}. \quad (22)$$

In this paper, we follow the discussion of Ref. [52] and adopt their expression for the chiral susceptibility at finite temperature

$$\begin{aligned}\chi^c = &4N_f T\sum_n\int\frac{\mathrm{d}^2 P}{(2\pi)^2}\times\Big\{\frac{[\varpi_n^2+P^2-B_n^2(P^2)]D_n(P^2)}{[\varpi_n+P^2+B_n^2(P^2)]^2}\\&-\frac{1}{\varpi_n^2+P^2}\Big\},\end{aligned} \quad (23)$$

where

$$D_n(P^2) = \frac{\partial B_n(P^2)}{\partial m}\Big|_{m \to 0}. \tag{24}$$

3 Numerical results

3.1 Retardation effects

Carrying out the integration of Eq. (20), we can get the momentum and frequency dependence of Π_A at different temperatures, as presented in Fig. 1. It is obvious, according to Eq. (20), that Π_A is an even function of frequency, so we choose only the positive frequencies. As we can see, the temporal part of vacuum polarization function varies both with momentum and frequency. The numerical result shows that Π_A increases as the absolute value of q_0 increases. Thus it has a minimum at zero frequency. At each frequency, $\Pi_A(q_0, \vec{q})$ approaches to a constant as the momentum decreases to zero. Comparing the momentum and frequency dependence of Π_A at different temperatures, the momentum dependence of Π_A has become less obvious, but the frequency dependence is not negligible. So from the point of Π_A, it is doubtful that the instantaneous exchange approximation is a good approximation at high temperature.
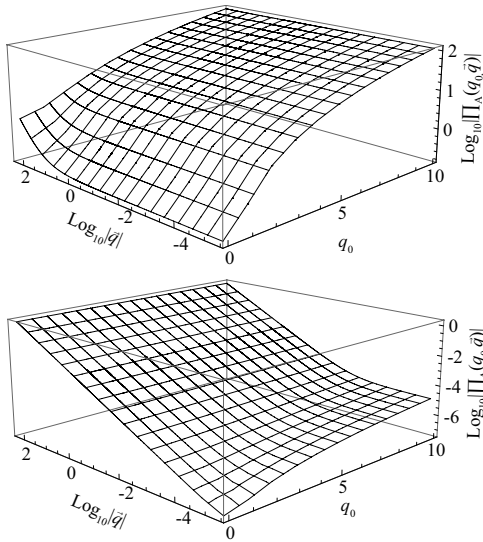

Fig. 1. Matsubara frequency q_0 and momentum $|\vec{q}|$ dependence of the vacuum polarization function $\Pi_{\mu\nu}(q_0, \vec{q})$ at a) $N_f = 1, T = 1. \times 10^3$ and b) $N_f = 1, T = 1$.

Subsequently, we calculate the fermion self-energy function $B(q_0, \vec{q})$. Theoretically, since we have considered the frequency dependence of the fermion self-energy function, we should take the summation on the left side of Eq. (18) from negative infinity to infinity. As a matter of fact, in the practical calculation, we have to take a cutoff. Since the zero frequency mode of $B(q_0, \vec{q})$ plays

a special role in investigating DCSB, we take the deviations of $B(0, \vec{q})$ for different frequency-cutoffs as the criterion.

When the deviation is less than a given value (namely 0.1%), we take the according frequency as the cutoff. Figure 2 shows how $B(0, \vec{q})$ varies as the frequency increases. Eventually the cutoff is set as 128 at $T = 10^{-3}$, and the numerical results converge to a stable curve. Also, it is worth mentioning that the cutoff is not universal, but depends on temperature. As the temperature increases, the proper frequency cutoff decreases.
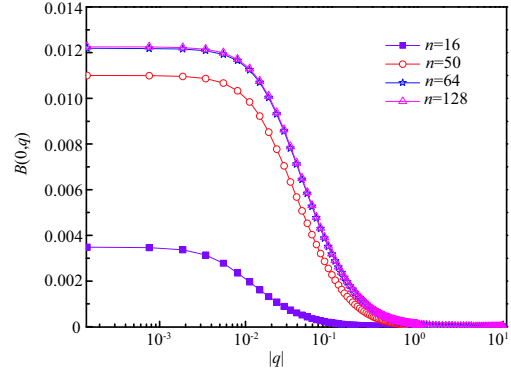

Fig. 2. (color online) Momentum dependence of $B(0, \vec{q})$ at different frequency cutoffs.
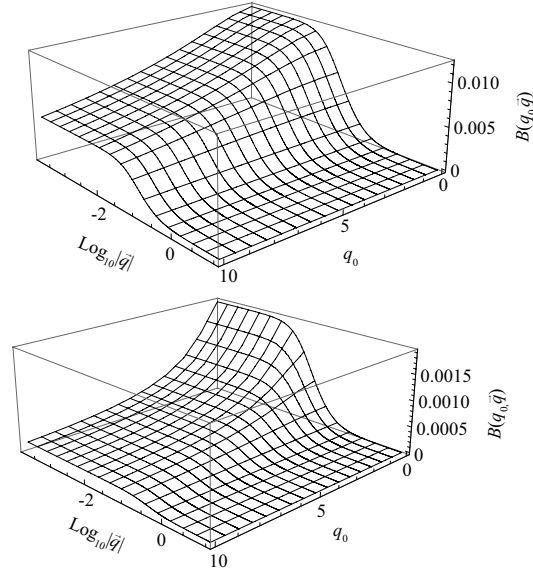

Fig. 3. Matsubara frequency q_0 and momentum $|\vec{q}|$ dependence of the fermion self-energy function $B(q_0, \vec{q})$ for $N_f = 1, T = 1. \times 10^{-3}$ and $N_f = 1, T = 4.6 \times 10^{-3}$.

By calculating the DSE of $B(q_0, \vec{q})$, we get the frequency and momentum dependence of the $B(q_0, \vec{q})$. They are presented in Figs. 3 and 4. The result shows that in the low momentum region the fermion self-energy $B(q_0, \vec{q})$ has a finite value and decreases slowly. Then

as the momentum increases, $B(q_0,\vec{q})$ decreases rapidly and approaches zero in the ultraviolet region. This is a common feature shared by all frequency modes. The main difference among the different modes is that in zero frequency mode, the fermion self-energy function has a maximum as shown in Fig. 3, and $B(q_0,\vec{q})$ diminishes as the frequency increases. We can see that this is true for different N_f.
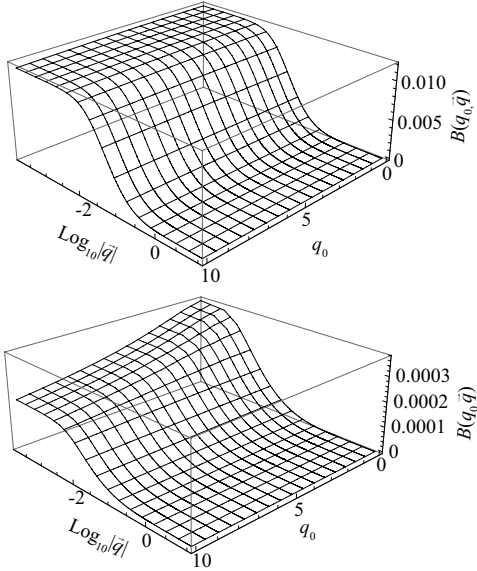

Fig. 4.   Matsubara frequency q_0 and momentum $|\vec{q}|$ dependence of the fermion self-energy function $B(q_0,\vec{q})$ for $N_f=1, T=1.\times10^{-4}$ and $N_f=2, T=1.\times10^{-4}$.

As the temperature increases, the magnitude of the fermion self-energy function quickly decreases and the spontaneously breaking symmetry gets restored at smaller momentum and frequency. This shows that spontaneous symmetry breaking is suppressed at finite temperature. From Fig. 3, we can see that, unlike the temperature effects, the effect of N_f is mainly in minimizing the scale of dynamical symmetry breaking.

As a check of our calculation, we take an approximation theoretically equivalent to the instantaneous approximation by just keeping the zero frequency part of Π_A, and calculate the DSE of $B(p)$. The results are shown in Fig. 5. As we can see, the two results are approximately the same. The small difference comes from the fact that we use a frequency cutoff instead of summing up to infinity and as the cutoff is increased, the difference tends to diminish. Combining Figs. 2 and 5, we find that the magnitude of the zero-mode fermion self-energy is much smaller than that obtained in the instantaneous approximation. $B(0,0)$ is just approximately one-tenth of the instantaneous approximation result, and $B(0,\vec{q})$ decreases to zero at smaller energy scale.

In some works, $B(0,\vec{q})$ is taken as an important criterion for spontaneous chiral symmetry breaking [36, 40]. In this sense, the magnitude of chiral symmetry breaking obtained here is much smaller than the one obtained in the instantaneous approximation, and the symmetry restoration happens at a much smaller energy scale.
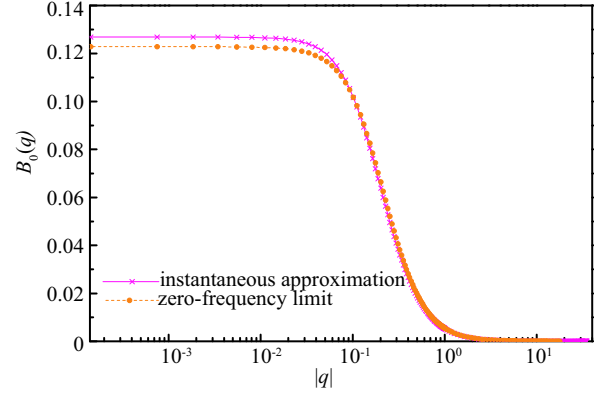

Fig. 5.   (color online) Momentum dependence of $B_0(\vec{q})$ for the instantaneous approximation results and the zero limit results.

3.2   Phase structure of QED₃

Substituting $B(q_0,\vec{q})$ into Eq. (22), we can get the explicit N_f and T dependence of $\langle\bar{\psi}\psi\rangle$. It is shown in Fig. 6. Also, we present the instantaneously approximation results as a comparison. The curves with fermion numbers labeled N_1 stand for the results considering the retardation effects and the N_2 curves stand for the instantaneous approximation results.

$$\langle\bar{\psi}\psi\rangle = -\frac{\partial\ln Z}{\partial m} = -\mathrm{T}\sum\!\!\!\!\!\!\int \mathrm{Tr}[S(p)]. \tag{25}$$

From Fig. 6, we can see that the chiral condensate $\langle\bar{\psi}\psi\rangle$ decreases slowly at low temperature, and quickly drops to zero as the temperature approaches a certain critical temperature. Comparing the instantaneous approximation results and those considering the retardation effects, we find that both show a decrease of the magnitude of spontaneous dynamical chiral symmetry breaking as the fermion flavor numbers increase. The difference is that the increase of N_f shows greater effects on the suppression of DCSB, which means the magnitude of the chiral condensate reduces more. Also, we can see that the critical temperature is much smaller than in the previous results. The results show that for a given number of fermion flavors N_f, the chiral condensate decreases slowly as the temperature increases; when the temperature arrives at the critical temperature T_c ($T_c=4.6\times10^{-3}$ for $N_f=1$, $T_c=2.2\times10^{-4}$ for $N_f=2$), the chiral condensate has a dramatic decrease and becomes zero as the temperature further increases.
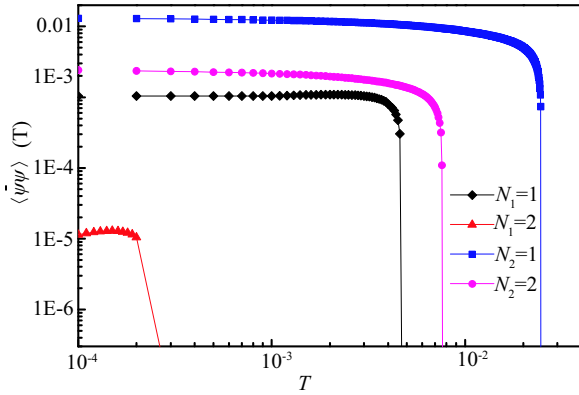
Fig. 6. (color online) Temperature dependence of chiral condensate (considering retardation effects).

In order to gain more knowledge of the chiral phase transition, we also calculated the chiral susceptibilities for different fermion flavors. The results are presented in Fig. 7. As we can see, the critical temperatures obtained from the calculation of chiral susceptibility are in accordance with the results of the chiral condensate. Meanwhile from the behavior of the chiral susceptibility, we can see that the chiral phase transition is of second order, in accordance with previous calculations [52].
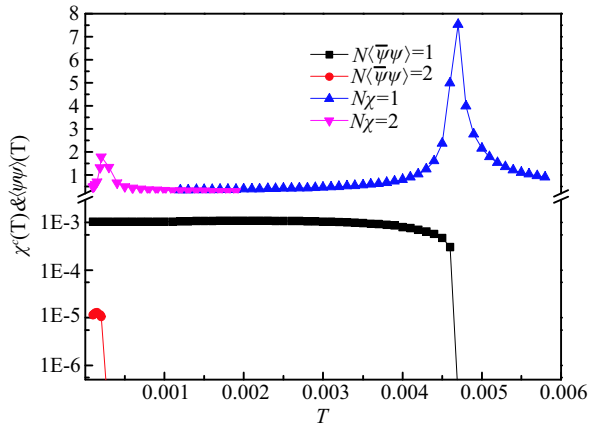

Fig. 7. (color online) Temperature dependence of chiral condensate and chiral susceptibility for different N_f.

Taking the zero temperature limit of Eq. (20), we can get $\Pi_A = \frac{\alpha}{8q}$, just the zero temperature case, and Eq. 5 degenerates back to Eq. (4) at $T \to 0$. Thus the critical N_f^c, for $T \to 0$, is $32/\pi^2$, the same value as in Ref. [25]. Subsequently, we get the phase diagram of the chiral phase transition in N_f-T_c space. The result is shown in Fig. 8. As we can see, there is a single critical line for N_f-T_c separating the chiral symmetry breaking phase from the chiral symmetry restored phase. Below the line, the chiral symmetry is spontaneously broken, and above the line,

chiral symmetry is restored. Only the $N_f \geqslant 0.667$ region is shown, but we find that as $T \to \infty$, N_f^c approaches 0. The increase of both T and N_f have the effect of suppressing the generation of dynamical masses, and the relation between T and N_f is nontrivial. According to the shape of the line, however, the effect of T and N_f is not equivalent. We can get this conclusion by comparing the phase diagram in Ref. [44] and Fig. 8.
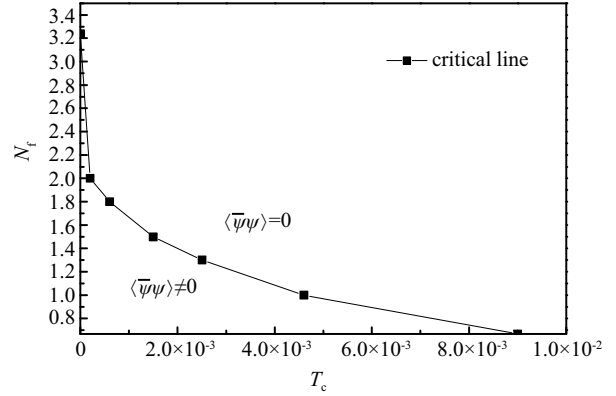

Fig. 8. Phase diagram for spontaneous chiral symmetry breaking in QED$_3$ in N_f-T_c space.

4   Summary and conclusions

In this paper, the dynamical symmetry breaking of QED$_3$ at finite temperature has been investigated in a gauge invariant truncation shceme. Many studies have been carried out in this framework, but they have mainly been done in the instantaneous approximation. We first expanded this work by considering the momentum and frequency dependence of the photon vacuum polarization function and fermion self-energy function at the same time, and found that the vacuum polarization function has an evident dependence on frequency, so the retardation effects may be non-negligible. Then we obtained the momentum and frequency dependence of the fermion self-energy function. Subsequently, the order parameter and chiral susceptibility of the chiral phrase transition for different temperatures and fermion flavors were calculated. The results show that with fermion flavor increasing, the dynamical chiral symmetry breaking gets suppressed just like for the zero temperature case.

Compared with previous results in the instantaneous approximation, the critical temperature obtained is much smaller and the scale of the chiral condensate is just one-tenth of the results of the instantaneous approximation. This shows that dynamical symmetry breaking as a low-energy phenomenon is not appropriate for investigation using the instantaneous approximation. Some recent works using a different method also gave a similar conclusion [53]. Finally, we gave the phase diagram of spontaneous symmetry breaking. It gives the region

in N_f-T_c space, where the spontaneously breaking chiral symmetry gets restored, and the line shows that the relation of T_c and N_f^c is nontrival.

We work in the QED$_3$ frame, and give a quantitative result for the impact of retardation effects on dynamic gap generation and chiral phase transition. The results show that the retardation effect plays a critical role in the finite temperature physics of QED$_3$, and temperature has in reality a greater effect on suppression the generation of mass gap. We expect this work will have practical application to novel two-dimension materials. This is a theoretical discussion without considering any practical material properties, such as graphene and other two-dimensional condensed systems.

References

1 C. D. Roberts and A. G. Williams, Prog. Part. Nucl. Phys., **33**: 477 (1994)
2 C. D. Roberts and S. M. Schmidt, Prog. Part. Nucl. Phys., **45,S1**: S1 - S103 (2000)
3 R. Alkofer and L. von Smekal, Phys. Rep., **353**: 281 (2001)
4 C. D. Roberts, M. S. Bhagwat, A. Höll, and S. V. Wright, Eur. Phys. J. Special Topics, **140**: 53 (2007)
5 P. A. Lee, N. Nagaosa, Xiao-Gang Wen, Rev. Mod. Phys., **78**: 17 (2006)
6 I. M. Affleck, and J. Brad, Phys. Rev. B, **37**: 3774 (1988)
7 L. B. Ioffe, A. I. Larkin, Phys. Rev. B, **39**: 8988 (1989)
8 D. H. Kim, P. A. Lee, Xiao-Gang Wen, Phys. Rev. Lett., **79**: 2109 (1997)
9 D. H. Kim, P. A. Lee, Annals of Physics, **272**: 130 (1999)
10 W. Rantner, Xiao-Gang Wen, Phys. Rev. Lett., **86**: 3871 (2001)
11 M. Franz, Z. Tešanović, Phys. Rev. Lett., **87**: 257003 (2001)
12 M. Franz, Z. Tešanović, and O. Vafek, Phys. Rev. B, **66**: 054535 (2002)
13 I. F. Herbut, Phys. Rev. Lett., **88**: 047006 (2002)
14 I. F. Herbut, Phys. Rev. B, **66**: 094504 (2002)
15 Guo-Zhu Liu, Geng Cheng, Phys. Rev. B, **66**: 100505 (2002)
16 Guo-Zhu Liu, Geng Cheng, Phys. Rev. D, **67**: 065010 (2003)
17 Guo-Zhu Liu, Wei Li, and Geng Cheng, Phys. Rev. B, **79**: 205429 (2009)
18 Jing-Rong Wang, Guo-Zhu Liu, New. J. Phys., **14**: 043036 (2012)
19 A. Katanin, Phys. Rev. B, **93**: 035132 (2016)
20 A. S. Mayorov, D. C. Elias, I. S. Mukhin, S. V. Morozov, L. A. Ponomarenko, K. S. Novoselov, A. K. Geim, and R. V. Gorbachev Nano. Lett., **12**: 4629 (2012)
21 S. G. Sharapov, V. P. Gusynin, and H. Beck, Phys. Rev. B, **69**: 075104 (2004)
22 A. Raya, E. D. Reyes, J. Phys. A, **41**: 355401 (2008)
23 Z. Tešanović, O. Vafek, and M. Franz, Phys. Rev. B, **65**: 180511 (2002)
24 A. A. Nersesyan, G. E. Vachnadze, J. Low. Temp. Phys., **77**: 293 (1989)
25 T. Appelquist, D. Nash, and L. C. R. Wijewardhana, Phys. Rev. Lett., **60**: 2575
26 D. Nash, Phys. Rev. Lett., **62**: 3024 (1989)
27 M. R. Pennington, D. Walsh, Phys. Lett. B, **253**: 246 (1991)
28 D. C. Curtis, M. R. Pennington, and D. Walsh, Phys. Lett. B, **295**: 313 (1992)
29 P. Maris, Phys. Rev. D, **54**: 4049 (1996)
30 R. Alkofer, W. Detmold, C. S. Fischer, and P. Maris, Phys. Rev. D, **70**: 014014 (2004)
31 S. Coleman, Comm. Math. Phys., **31**: 259 (1973)
32 N. D. Mermin, H. Wagner, Phys. Rev. Lett., **17**: 1133 (1966)
33 R. J. Cava, B. Batlogg, R. B. van Dover, J. J. Krajewski, J. V. Waszczak, R. M. Fleming, W. F. Peck, L. W. Rupp, P. Marsh, A. C. W. P. James, and L. F. Schneemeyer, Nature, **345**: 602 (1990)
34 Elbio Dagotto, Rev. Mod. Phys., **66**: 763 (1994)
35 K. Aleksandar, Phys. Lett. B, **189**: 449 (1987)
36 N. Dorey, N. E. Mavromatos, Phys. Lett. B, **266**: 163 (1991)
37 N. Dorey, N. E. Mavromatos, Nucl. Phys. B, **386**: 614 (1992)
38 I. J. R. Aitchison, M. Klein-Kreisler, Phys. Rev. D, **50**: 1068 (1994)
39 Ian Johnston Rhind Aitchison, Zeitschrift für Physik C Particles, Fields, **67**: 303 (1995)
40 I. J. R. Aitchison, N. Dorey, M. Klein-Kreisler, and N. E. Mavromatos, Phys. Lett. B, **294**: 91 (1992)
41 Hong-tao Feng, Bin Wang, Wei-min Sun, and Hong-shi Zong, Eur. Phys. J. C, **73**: 2444 (2013)
42 Hong-tao Feng, Yu-qing Zhou, Pei-Lin Yin, and Hong-shi Zong, Phys. Rev. D, **88**: 125022 (2013)
43 Pei-lin Yin, Yuan-mei Shi, Zhu-fang Cui, Hong-tao Feng, and Hong-shi Zong, Phys. Rev. D, **90**: 036007 (2014)
44 Pei-Lin Yin, Wei Wei, Hai-Xiao Xiao, Hong-Tao Feng, Xiao-Jun Liu, and Hong-Shi Zong, Phys. Rev. D, **93**: 016009 (2016)
45 G. Triantaphyllou, Phys. Rev. D, **58**: 065006 (1998)
46 L. O. Nascimento, van Sérgio Alves, F. Peña, C. M. Smith, and E. C. Marino, Phys. Rev. D, **92**: 025018 (2015)
47 F. Karsch, E. Laermann, Phys. Rev. D, **50**: 6954 (1994)
48 M. Cheng, N. H. Christ, M. A. Clark, J. van der Heide, C. Jung, F. Karsch, O. Kaczmarek, E. Laermann, R. D. Mawhinney, C. Miao, P. Petreczky, K. Petrov, C. Schmidt, W. Soeldner, and T. Umeda, Phys. Rev. D, **75**: 034506 (2007)
49 Liang-Kai Wu, Xiang-Qian Luo, and He-Sheng Chen, Phys. Rev. D, **76**: 034505 (2007)
50 Hong-tao Feng, Bin Wang, Wei-min Sun, and Hong-shi Zong, Phys. Rev. D, **86**: 105042 (2012)
51 Zhu-Fang Cui, Feng-Yao Hou, Yuan-Mei Shi, Yong-Long Wang, and Hong-Shi Zong, Annals of Physics, **358**: 172 (2015)
52 Hongtao Feng, Song Shi, Peilin Yin, and Hongshi Zong, Phys. Rev. D, **86**: 065002 (2012)
53 P. M. Lo, E. S. Swanson, Phys. Rev. D, **89**: 025015 (2014)